Letter

http://justc.ustc.edu.cn

Received: January 23, 2024; Accepted: April 02, 2024

Large and nonlinear electric field response in a two-dimensional ferroelectric Rashba material

Li Sheng[1,2*], Xiaomin Fu[1,2*], Chao Jia[1,2], Xingxing Li[1,2,3,4] ✉, and Qunxiang Li[1,2,3,4] ✉

[1]*Key Laboratory of Precision and Intelligent Chemistry, University of Science and Technology of China, Hefei 230026, China;*
[2]*Department of Chemical Physics, University of Science and Technology of China, Hefei 230026, China;*
[3]*Hefei National Research Center for Physical Sciences at the Microscale, University of Science and Technology of China, Hefei 230026, China;*
[4]*Hefei National Laboratory, University of Science and Technology of China, Hefei 230088, China*

* These authors contributed equally to this work
✉Correspondence: Xingxing Li, E-mail: lixx@ustc.edu.cn; Qunxiang Li, E-mail: liqun@ustc.edu.cn
© 2024 The Author(s). This is an open access article under the CC BY-NC-ND 4.0 license (http://creativecommons.org/licenses/by-nc-nd/4.0/).

Graphical abstract

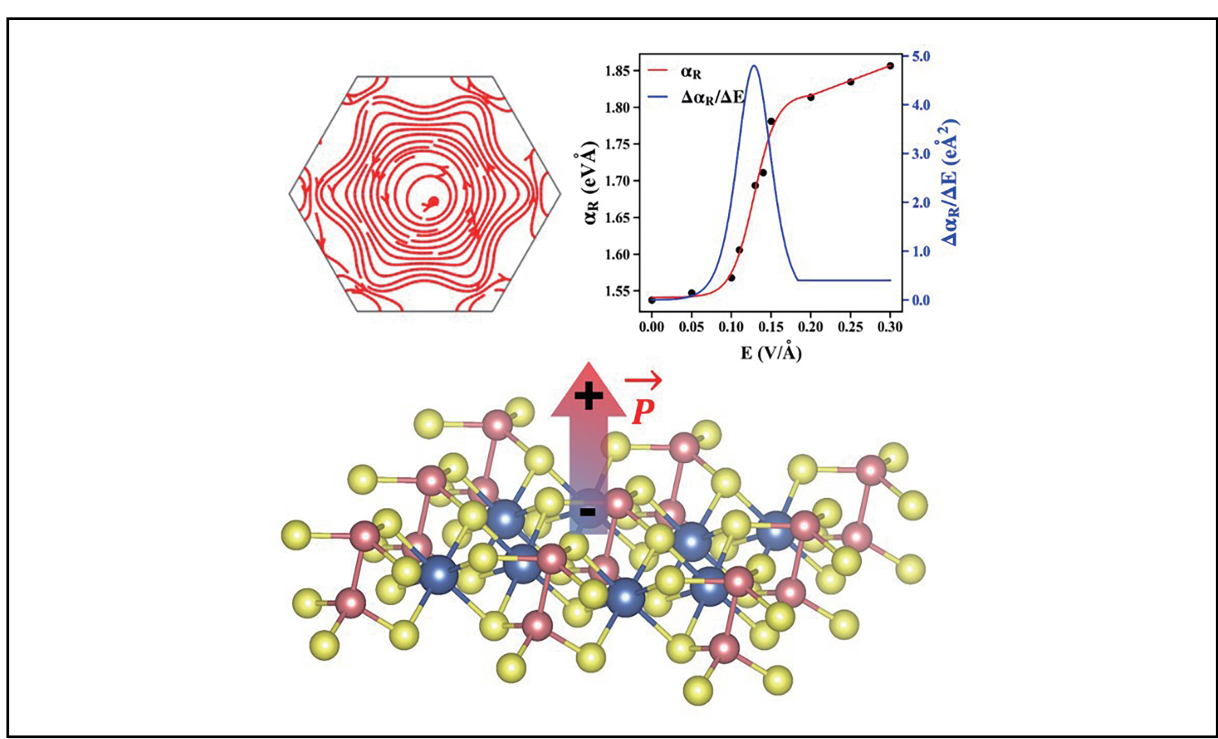

To date, monolayer YSbTe3 has been identified as a ferroelectric Rashba semiconductor with the largest electric field response.

Public summary

- This work designs a thermodynamically stable two-dimensional Rashba semiconductor, $YSbTe_3$, with an indirect band gap of 1.04 eV, a large Rashba constant of 1.54 eV·Å, and a strong electric field response up to 4.80 e·Å².
- $YSbTe_3$ exhibits an unusual nonlinear relationship between the Rashba constant and the electric field, and the Rashba spin texture of $YSbTe_3$ can be reversed by changing the electric polarization direction.
- These properties make the ferroelectric Rashba semiconductor $YSbTe_3$ quite a promising candidate for spintronic applications.

Citation: Sheng L, Fu X M, Jia C, et al. Large and nonlinear electric field response in a two-dimensional ferroelectric Rashba material. *JUSTC*, **2024**, 54(6): 0602. DOI: 10.52396/JUSTC-2024-0004

JUSTC

Letter

http://justc.ustc.edu.cn

Received: January 23, 2024; Accepted: April 02, 2024

Large and nonlinear electric field response in a two-dimensional ferroelectric Rashba material

Li Sheng[1,2*], Xiaomin Fu[1,2*], Chao Jia[1,2], Xingxing Li[1,2,3,4] ✉, and Qunxiang Li[1,2,3,4] ✉

[1]Key Laboratory of Precision and Intelligent Chemistry, University of Science and Technology of China, Hefei 230026, China;
[2]Department of Chemical Physics, University of Science and Technology of China, Hefei 230026, China;
[3]Hefei National Research Center for Physical Sciences at the Microscale, University of Science and Technology of China, Hefei 230026, China;
[4]Hefei National Laboratory, University of Science and Technology of China, Hefei 230088, China

* These authors contributed equally to this work
✉Correspondence: Xingxing Li, E-mail: lixx@ustc.edu.cn; Qunxiang Li, E-mail: liqun@ustc.edu.cn

© 2024 The Author(s). This is an open access article under the CC BY-NC-ND 4.0 license (http://creativecommons.org/licenses/by-nc-nd/4.0/).

Cite This: *JUSTC*, **2024**, 54(6): 0602 (5pp)

Abstract: The achievement of electrical spin control is highly desirable. One promising strategy involves electrically modulating the Rashba spin orbital coupling effect in materials. A semiconductor with high sensitivity in its Rashba constant to external electric fields holds great potential for short channel lengths in spin field-effect transistors, which is crucial for preserving spin coherence and enhancing integration density. Hence, two-dimensional (2D) Rashba semiconductors with large Rashba constants and significant electric field responses are highly desirable. Herein, by employing first-principles calculations, we design a thermodynamically stable 2D Rashba semiconductor, $YSbTe_3$, which possesses an indirect band gap of 1.04 eV, a large Rashba constant of 1.54 eV·Å and a strong electric field response of up to 4.80 e·Å^2. In particular, the Rashba constant dependence on the electric field shows an unusual nonlinear relationship. At the same time, $YSbTe_3$ has been identified as a 2D ferroelectric material with a moderate polarization switching energy barrier (~ 0.33 eV per formula). By changing the electric polarization direction, the Rashba spin texture of $YSbTe_3$ can be reversed. These outstanding properties make the ferroelectric Rashba semiconductor $YSbTe_3$ quite promising for spintronic applications.

Keywords: computational chemistry; Rashba effect; ferroelectrics; spintronics

CLC number: O469 **Document code:** A

1 Introduction

The Rashba effect, which originates from structural inversion asymmetry (SIA), represents a typical spin–orbit coupling (SOC) phenomenon and offers a potent means for spin transport and electrical spin control[1]. The critical feature of Rashba SOC is that moving electrons experience an effective magnetic field driving the precession of the spin orientation of the electrons[2,3]. In recent decades, the Rashba effect has undergone extensive exploration in diverse systems, including oxide interfaces[4], topological insulators[5], semiconductor quantum wells[6], alloy surfaces and heavy atoms[7], perovskite-structured compounds[8], and low-dimensional nanomaterials[9]. In addition, Rashba effect-based spintronic devices have emerged, a prominent example of which is the spin field effect transistor (SFET)[10]. Due to the Rashba SOC, electron spins precess around the effective magnetic field in the SFET[11]. SFETs have been experimentally demonstrated in 2D semiconductor quantum well systems[12,13].

To date, a variety of 2D Rashba semiconductors have been proposed, e.g., 2D $AlBiS_3$[14], AlBi[15], $SrTiO_3$ and $LaAlO_3$[16], Bi*TeX* (X = I and Br) monolayers[17], and Bi/Ag/CoFeB trilayers[18]. To design high-performance SFETs, Rashba materials must have a large Rashba constant α_R and a significant electric field response $|\Delta\alpha_R/\Delta E|$[19]. This phenomenon entails large spin splitting, particularly in the conduction band (CB) or valence band (VB). Moreover, it is crucial that the Rashba constant α_R exhibits a sensitive response to the electric field, allowing for modulation of the spin precession angle (θ) via the electric field, based on the equation $\Delta\theta = 2m^*\Delta\alpha_R L/\hbar^2$, where L denotes the channel length of the SFET and m^* represents the effective mass of the carriers. In previously reported representative Rashba materials such as T-$RbPbI_3$[10], BiSb[19], and $MAPbI_3$ ($MA=CH_3NH_3$)[20], their Rashba constants vary linearly with the electric field, with $|\Delta\alpha_R/\Delta E|$ values of 0.44, 0.92, and 1.95 e·Å^2, respectively[10,19,20]. Searching for 2D Rashba materials with stronger electric field responses remains a pending and challenging task.

Here, the transition metal phosphorus trichalcogenide $FePS_3$ is selected as the structural prototype, and Fe, P and S are replaced by other elements. Specifically, we replace Fe with nonmagnetic elements, namely, Al, Bi, Ga, In, Os, Ru, Sb, Sc, and Y; substitute group VI elements, including N, Sb, As, and Bi, for P; and replace S with the chalcogens Se and Te. Eventually, 2D $YSbTe_3$, which exhibits the largest electric field response and a large Rashba constant, is screened out compared with the literature. Moreover, 2D $YSbTe_3$ has also been shown to be a novel ferroelectric Rashba semiconductor, where the spin texture can be reversed through the inversion of ferroelectric polarization.

DOI: 10.52396/JUSTC-2024-0004
JUSTC, **2024**, 54(6): 0602

2 Computational methods

The calculations in this study were conducted utilizing density functional theory (DFT) implemented in the Vienna ab initio simulation package (VASP)[21]. The projector augmented wave (PAW) method[22] and the generalized gradient approximation of the Perdew-Burke-Ernzerhof (GGA-PBE) functional were applied[23]. The plane-wave cutoff energy was set to 500 eV. Lattice constants and atomic structures were fully relaxed until the convergence of energy and force was less than 10^{-6} eV and 0.01 eV·Å^{-1}, respectively. A 7×7×1 *k*-point sampling mesh grid was employed for the structure optimization and calculation of the electronic properties. The vacuum layer length was set to 20.0 Å in the *z*-direction. Considering van der Waals (vdW) interactions, the DFT-D3 method was employed[24]. The investigation of Rashba spin splitting incorporated the effect of SOC. The electronic band structures were calculated using the HSE06 hybrid functional since the PBE functional generally underestimates the band gap[25]. To investigate the dynamic stability of 2D $YSbTe_3$, the phonon spectrum was calculated with a 3×3×1 supercell via the finite difference method facilitated by the phonopy package interfaced with VASP[26,27]. Additionally, the solid-state nudged elastic band (SS-NEB) method was used for calculating the ferroelectric polarization switching process[28]. Ab initio molecular dynamics simulations were performed to investigate the thermal stability of 2D $YSbTe_3$. The simulation was controlled by a Nosé–Hoover thermostat and executed for a 3×3×1 supercell with a time step of 1.0 fs at 500 K.

3 Results and discussion

3.1 Geometry structures and stability

Fig. 1a illustrates that 2D $YSbTe_3$ possesses a noncentrosymmetric structure with *P*31*m* symmetry. The optimized lattice parameters for $YSbTe_3$ are $a = b = 7.56$ Å. The formation energy (E_f) of $YSbTe_3$ is calculated to be −2.02 eV per formula unit using $E_f(YSbTe_3) = E(YSbTe_3)\text{-}E(Y)\text{-}E(Sb)\text{-}3E(Te)$, where $E(YSbTe_3)$, E(Y), E(Sb), and E(Te) indicate the energies of 2D $YSbTe_3$, bulk Y, Sb and Te in their most stable phases, respectively. This formation energy is on the same order of magnitude as that of 2D $CsSnCl_3$ (−2.28 eV per formula unit)[10] synthesized experimentally[29], indicating the good stability of this ternary compound. The phonon spectrum shown in Fig. 1b presents no imaginary frequency, which affirms the dynamic stability of the 2D $YSbTe_3$. To further assess its thermal stability, ab initio molecular dynamics simulations were performed. As illustrated in Fig. S1, the structure of 2D $YSbTe_3$ can be retained at 500 K, with both the temperature and total energy fluctuating around their equilibrium values.

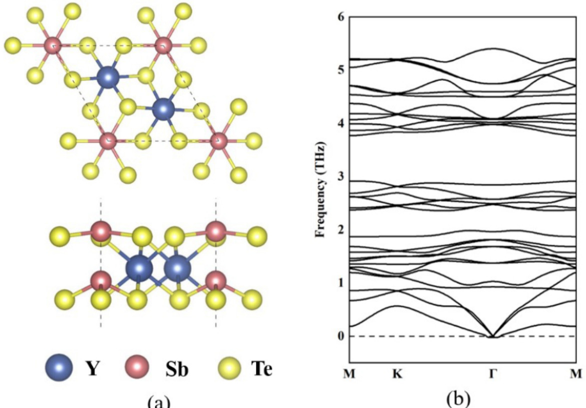

Fig. 1. (a) Top and side views of the structure of 2D $YSbTe_3$. The Y, Sb, and Te atoms are represented by blue, red, and yellow balls, respectively. (b) Phonon spectrum of $YSbTe_3$.

3.2 Electronic structures

Then, we investigated the electronic properties of $YSbTe_3$. Fig. 2a and b depict the electronic band structures of $YSbTe_3$, which were calculated by using the HSE06 and HSE06 + SOC methods, respectively. The 2D $YSbTe_3$ demonstrates the characteristics of a nonmagnetic semiconductor, featuring an indirect bandgap of 1.19 eV without considering the SOC. The band gap with the SOC is slightly smaller, decreasing to 1.04 eV. Furthermore, the valence band of 2D $YSbTe_3$ displays significant Rashba spin splitting with lifted spin degeneracies, i.e., the VB (red) and VB−1 (blue) bands are differentiated by momentum-dependent energy splitting $\Delta E=2\alpha_R k$ induced by the Rashba SOC. The time-reversal symmetry of the system makes the VB and VB−1 bands contact the Γ-point. The electronic band structures computed using the PBE and PBE+SOC methods are also shown in Fig. S2 and are similar to those of the HSE06 and HSE06 + SOC results. Fig. 2c, d illustrates the spin textures of VB and VB−1 in the hexagonal reciprocal space. The inner branch VB−1 exhibits a clockwise spin texture, while the outer branch VB shows a counterclockwise spin texture. Notably, the VB exhibits significant Rashba splitting, and the Rashba constant α_R is determined to be 1.54 eV·Å according to the equation $\alpha_R=2E_R/k_R$ (see the Supporting information for more details of the formula derivation for the Rashba model).

3.3 Tunable Rashba spin splitting

To investigate the electric field response $|\Delta\alpha_R/\Delta E|$, we applied external positive and negative electric fields perpendicular to the atomic plane of 2D $YSbTe_3$. It is worth noting that the VB keeps a typical Rashba splitting under a positive electric field, whereas it is not completely split when subjected to a negative electric field (Fig. S3). The Rashba constant (α_R) presents a nonlinear relationship with increasing positive electric field (E), as depicted by the red line in Fig. 3. The nonlinear relationship between E and α_R is characterized by an S-shaped curve, i.e., a gradual increase, a steep increase, and a slow increase as E increases. Consequently, the electric field response $|\Delta\alpha_R/\Delta E|$ also changes with the electric field (the blue line in Fig. 3). When E reaches 0.13 V·Å^{-1}, $|\Delta\alpha_R/\Delta E|$ attains a peak value of 4.80 e·Å^2, surpassing that of other Rashba semiconductors reported in previous literature[10,19,20].

To explore why the relationship between the electric field E and Rashba constant α_R of $YSbTe_3$ is nonlinear, we analyzed the orbital composition of $YSbTe_3$ under electric fields of 0 V·Å^{-1} and 0.3 V·Å^{-1} according to the density of states (DOS), as displayed in Fig. S4**.** We find that the DOS under

DOI: 10.52396/JUSTC-2024-0004
JUSTC, **2024**, 54(6): 0602

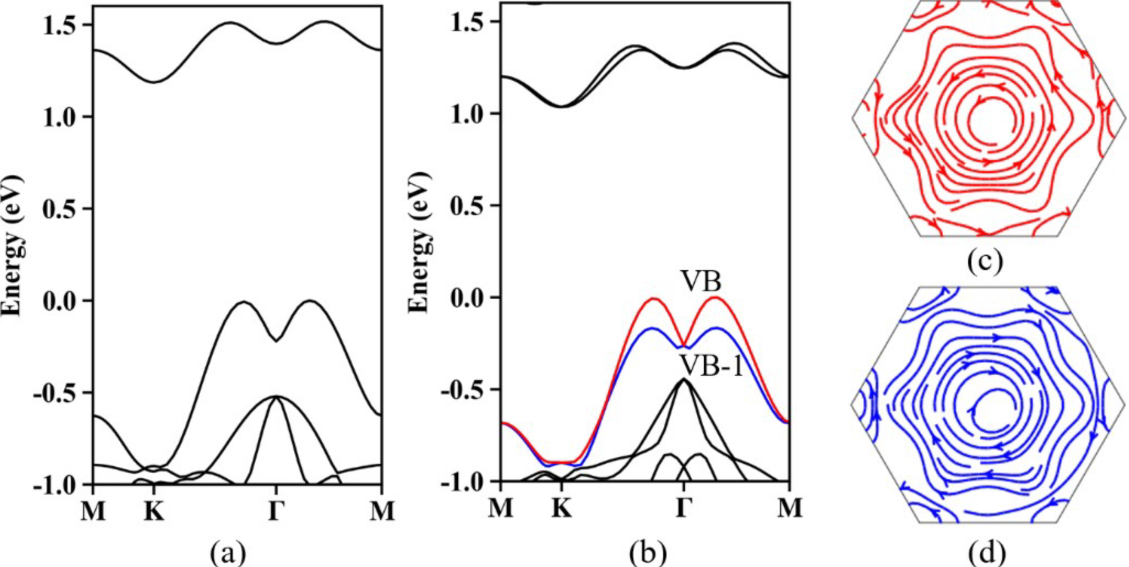

Fig. 2. (a, b) Band structures of 2D $YSbTe_3$ calculated with HSE06 and HSE06+SOC, respectively. VB and VB−1 are shown in red and blue, respectively. The characteristic spin texture structures of (c) VB and (d) VB−1 calculated with the HSE06 + SOC functional. The Fermi levels are set to zero.

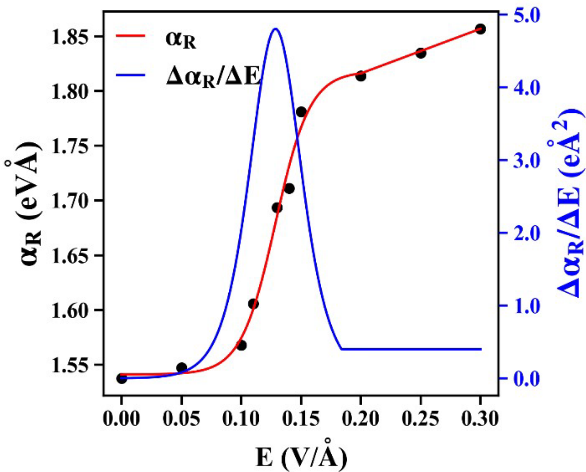

Fig. 3. The relationship between the Rashba constant and the electric field (red line and black dots, left *y*-axis) and the corresponding electric field response of the Rashba constant ($|\Delta\alpha_R/\Delta E|$) (blue line, right *y*-axis) for 2D $YSbTe_3$.

electric fields of 0 V·Å^{-1} and 0.3 V·Å^{-1} are nearly identical. In both cases, the VB bands are mainly attributed to the p_y and p_z orbitals of the Te element. Therefore, the variation in the electric field has no effect on the orbital composition. On the other hand, we investigated the correlation between the band gap (E_g) and the electric field of $YSbTe_3$ (Fig. S5) and compared it with the relationship between the Rashba constant and the electric field. It is clear that the variation trend of E_g with respect to E is the opposite of that of α_R, i.e., a nonlinear, inverse S-shaped curve is formed. As previously reported, α_R is negatively correlated with E_g[30,31], indicating that as the band gap decreases, the Rashba constant increases. Therefore, the nonlinear electric field response of the Rashba constant originates from the nonlinear variation in the band gap of $YSbTe_3$ with the electric field. To understand the nonlinear behavior of the band gap, the charge density distributions of the VB and CB were analyzed. As shown in Fig. S6a, the VB of $YSbTe_3$ is primarily contributed by the Te atoms in the upper surface layer, while CB is mainly constructed by the Te atoms in both the upper and lower surface layers. Thus, the center of charge for the VB is located at a greater position than that for the CB. When a positive electric field is applied, the electrostatic potential energy of the VB is greater than that of the CB. That is, with increasing electric field, the energy level of the VB moves upward relative to the CB level, resulting in a linear reduction in the band gap (note that the electrostatic potential energy is a linear function of the electric field). However, such a conclusion is based on the assumption that the charge distributions of the VB and CB remain unchanged under an external electric field. In fact, we observe significant charge transfer between the upper and lower Te atoms. Moreover, such charge transfer is nonlinear with respect to the electric field (Fig. S6b). This may be the reason for the nonlinear variation in the band gap in 2D $YSbTe_3$. We note that nonlinearity in the band gap variation with the electric field also occurs in bilayer $MoSi_2N_4$, WSi_2N_4, and graphene[32,33].

3.4 Ferroelectric properties

To date, 2D ferroelectric materials have garnered great interest, given that bulk ferroelectric materials tend to lose their ferroelectric polarization below a critical thickness due to the depolarizing electrostatic field and finite size effect. The calculation of the double-well potential with two degenerated ferroelectric states indicates the ferroelectric characteristics of $YSbTe_3$ (Fig. 4). The two ferroelectric states exhibit opposing ferroelectric polarization directions, which can be interconverted through atomic position deformations, specifically the upward or downward movement of Sb atoms. The switching energy barrier is determined to be 0.33 eV per formula

DOI: 10.52396/JUSTC-2024-0004
JUSTC, **2024**, 54(6): 0602

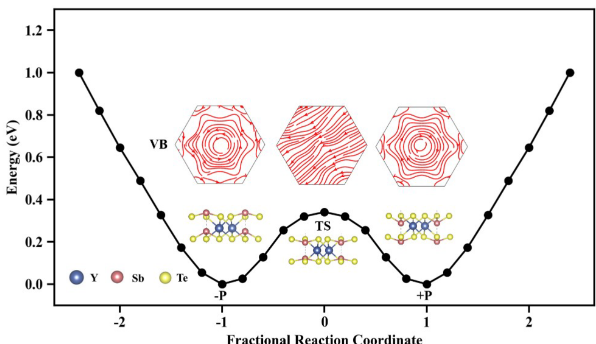

Fig. 4. Double-well potential vs. atomic displacement along the *z*-axis. The energy of the ferroelectric state is taken as a reference. The VB spin textures of two degenerated ferroelectric states and one transition state (TS) are displayed.

unit, with the transition state (TS) being the paraelectric phase. The phonon dispersion for the paraelectric phase ($P\bar{3}1m$) is shown in Fig. S7. Clearly, there is an imaginary, soft optical mode (λ) present in the phonon spectrum, while the ferroelectric phase has no soft mode (Fig. 1). As the temperature decreases below the critical temperature, the paraelectric phase evolves into the ferroelectric phase, and the soft mode is stabilized by symmetry breaking. In such a paraelectric state, where Sb atoms are symmetrically distributed in the plane of Y atoms, $YSbTe_3$ lacks the Rashba effect, as evidenced by the absence of clockwise and counterclockwise rotations in the spin texture of the VB (Fig. 4). Importantly, the spin textures of the two ferroelectric states are found to be opposite, i.e., the direction of the spin texture is reversed along with ferroelectric polarization switching. In addition, the electric polarization of 2D $YSbTe_3$ is calculated to be 2.91×10^{-12} $C\cdot m^{-1}$, which is comparable to that of other 2D ferroelectric materials in the literature (see Table S1). Thus, 2D $YSbTe_3$ is identified as a ferroelectric Rashba material.

4 Conclusions

In summary, $YSbTe_3$ is theoretically confirmed as a potential candidate for a 2D ferroelectric Rashba material. On the one hand, 2D $YSbTe_3$ shows a nonlinear relationship between the electric field and the Rashba constant α_R. The electric field response parameter $|\Delta\alpha_R/\Delta E|$ for $YSbTe_3$ is determined to be 4.80 $e\cdot Å^2$, the largest among all 2D Rashba semiconductors, which is highly promising for designing highly integrated SFETs. However, $YSbTe_3$ is also ferroelectric. Ferroelectric polarization switching can reverse the Rashba spin texture.

Supporting information

The supporting information for this article can be found online at https:// doi.org/10.52396/JUSTC-2024-0004. Ab initio molecular dynamics simulations, projected density of states, electronic band structures calculated via the PBE and PBE + SOC methods, band structures when applying positive and negative electric fields, phonon spectrum of the paraelectric phase, charge density of the valence band and conduction band, variation in the Rashba constant, bandgap, charge of Te atoms with positive electric fields, and comparison of the electric polarization of 2D $YSbTe_3$ with that of other 2D ferroelectric materials are provided in the supporting information.

Acknowledgements

This work was supported by the National Natural Science Foundation of China (22322304, 22273092, 22373095), the Strategic Priority Research Program of the Chinese Academy of Sciences (XDB0450101), the Innovation Program for Quantum Science and Technology (2021ZD0303306), and the USTC Tang Scholar. The authors wish to acknowledge the Supercomputing Center of the USTC for providing computational resources.

Conflict of interest

The authors declare that they have no conflict of interest.

Biographies

Li Sheng is currently a graduate student in the Department of Chemical Physics, University of Science and Technology of China, under the supervision of Prof. Qunxiang Li. His research mainly focuses on computer simulations of catalytic and magnetic properties of two-dimensional materials.

Xiaomin Fu is currently a graduate student in the Department of Chemical Physics, University of Science and Technology of China, under the supervision of Prof. Qunxiang Li. Her research mainly focuses on computer simulations of two-dimensional Rashba materials.

Xingxing Li is a Professor in the Department of Chemical Physics, University of Science and Technology of China (USTC). He received his Ph.D. degree in Physical Chemistry from USTC in 2015. His research mainly focuses on the first-principles studies of low-dimensional spintronic materials and molecular devices.

Qunxiang Li is a Professor in the Department of Chemical Physics, University of Science and Technology of China (USTC). He received his Ph.D. degree in Condensed Matter Physics from USTC in 1999. His research mainly focuses on single molecule chemical physics, molecular electronics, and computational materials science.

References

[1] Chen J J, Wu K, Hu W, et al. Spin–orbit coupling in 2D semiconductors: a theoretical perspective. *J. Phys. Chem. Lett.*, **2021**, *12* (51): 12256–12268.
[2] Koo H C, Kim S B, Kim H, et al. Rashba effect in functional spintronic devices. *Adv. Mater.*, **2020**, *32* (51): 2002117.
[3] Lee S, Koike H, Goto M, et al. Synthetic Rashba spin–orbit system using a silicon metal-oxide semiconductor. *Nat. Mater.*, **2021**, *20* (9): 1228–1232.
[4] Lin W, Li L, Doğan F, et al. Interface-based tuning of Rashba spin-orbit interaction in asymmetric oxide heterostructures with 3d electrons. *Nat. Commun.*, **2019**, *10* (1): 3052.
[5] Lyu J K, Ji W X, Zhang S F, et al. Strain-tuned topological insulator and Rashba-induced anisotropic momentum-locked Dirac cones in two-dimensional SeTe monolayers. *ACS Appl. Mater. Interfaces*, **2018**, *10* (50): 43962–43969.
[6] Ciocys S T, Maksimovic N, Analytis J G, et al. Driving ultrafast spin and energy modulation in quantum well states via photo-induced

electric fields. *npj Quantum Mater.*, **2022**, *7* (1): 79.

[7] Jolie W, Hung T C, Niggli L, et al. Creating tunable quantum corrals on a Rashba surface alloy. *ACS Nano*, **2022**, *16* (3): 4876–4883.

[8] Lafalce E, Amerling E, Yu Z G, et al. Rashba splitting in organic–inorganic lead–halide perovskites revealed through two-photon absorption spectroscopy. *Nat. Commun.*, **2022**, *13* (1): 483.

[9] Lee S, Kwon Y K. Unveiling giant hidden rashba effects in two-dimensional Si_2Bi_2. *npj 2D Mater. Appl.*, **2020**, *4* (1): 45.

[10] Chen J J, Wu K, Hu W, et al. Tunable Rashba spin splitting in two-dimensional polar perovskites. *J. Phys. Chem. Lett.*, **2021**, *12* (7): 1932–1939.

[11] Datta S, Das B. Electronic analog of the electro-optic modulator. *Appl. Phys. Lett.*, **1990**, *56* (7): 665–667.

[12] Park Y H, Choi J W, Kim H J, et al. Complementary spin transistor using a quantum well channel. *Sci. Rep.*, **2017**, *7* (1): 46671.

[13] Chuang P, Ho S C, Smith L W, et al. All-electric all-semiconductor spin field-effect transistors. *Nat. Nanotechnol.*, **2015**, *10* (1): 35–39.

[14] Fu X M, Jia C, Sheng L, et al. Bipolar Rashba semiconductors: a class of nonmagnetic materials for electrical spin manipulation. *J. Phys. Chem. Lett.*, **2023**, *14* (50): 11292–11297.

[15] Chen J J, Wu K, Hu W, et al. High-throughput inverse design for 2D ferroelectric Rashba semiconductors. *J. Am. Chem. Soc.*, **2022**, *144* (43): 20035–20046.

[16] Song Q, Zhang H R, Su T, et al. Observation of inverse Edelstein effect in Rashba-split 2DEG between $SrTiO_3$ and $LaAlO_3$ at room temperature. *Sci. Adv.*, **2017**, *3* (3): e1602312.

[17] Qu J, Han X, Sakamoto S, et al. Reversal of spin-polarization near the fermi level of the Rashba semiconductor BiTeCl. *npj Quantum Mater.*, **2023**, *8* (1): 13.

[18] Nakayama H, Kanno Y, An H, et al. Rashba-Edelstein magnetoresistance in metallic heterostructures. *Phys. Rev. Lett.*, **2016**, *117* (11): 116602.

[19] Wu K, Chen J J, Ma H H, et al. Two-dimensional giant tunable Rashba semiconductors with two-atom-thick buckled honeycomb structure. *Nano Lett.*, **2021**, *21* (1): 740–746.

[20] Liu B C, Gao H X, Meng C Y, et al. The impact of an external electric field on the Rashba effect in two-dimensional hybrid perovskites. *J. Mater. Chem. C*, **2023**, *11* (30): 10370–10376.

[21] Kresse G, Furthmüller J. Efficient iterative schemes for *ab initio* total-energy calculations using a plane-wave basis set. *Phys. Rev. B*, **1996**, *54* (16): 11169–11186.

[22] Blöchl P E. Projector augmented-wave method. *Phys. Rev. B*, **1994**, *50* (24): 17953–17979.

[23] Perdew J P, Burke K, Ernzerhof M. Generalized gradient approximation made simple. *Phys. Rev. Lett.*, **1996**, *77* (18): 3865–3868.

[24] Grimme S, Antony J, Ehrlich S, et al. A consistent and accurate *ab initio* parametrization of density functional dispersion correction (DFT-D) for the 94 elements H-Pu. *J. Chem. Phys.*, **2010**, *132* (15): 154104.

[25] Heyd J, Scuseria G E, Ernzerhof M. Hybrid functionals based on a screened Coulomb potential. *J. Chem. Phys.*, **2003**, *118* (18): 8207–8215.

[26] Alfè D. PHON: A program to calculate phonons using the small displacement method. *Comput. Phys. Commun.*, **2009**, *180* (12): 2622–2633.

[27] Togo A, Chaput L, Tadano T, et al. Implementation strategies in phonopy and phono3py. *J. Phys. : Condens. Matter*, **2023**, *35* (35): 353001.

[28] Sheppard D, Xiao P, Chemelewski W, et al. A generalized solid-state nudged elastic band method. *J. Chem. Phys.*, **2012**, *136* (7): 074103.

[29] Ali M S, Das S, Abed Y F, et al. Lead-free $CsSnCl_3$ perovskite nanocrystals: rapid synthesis, experimental characterization and DFT simulations. *Phys. Chem. Chem. Phys.*, **2021**, *23* (38): 22184–22198.

[30] Bahramy M S, Arita R, Nagaosa N. Origin of giant bulk Rashba splitting: Application to BiTeI. *Phys. Rev. B*, **2011**, *84* (4): 041202.

[31] Gupta S, Yakobson B I. What dictates Rashba splitting in 2D van der Waals heterobilayers. *J. Am. Chem. Soc.*, **2021**, *143* (9): 3503–3508.

[32] Wu Q, Cao L, Ang Y S, et al. Semiconductor-to-metal transition in bilayer $MoSi_2N_4$ and WSi_2N_4 with strain and electric field. *Appl. Phys. Lett.*, **2021**, *118* (11): 113102.

[33] Nourbakhsh A, Agarwal T K, Klekachev A, et al. Chemically enhanced double-gate bilayer graphene field-effect transistor with neutral channel for logic applications. *Nanotechnology*, **2014**, *25* (34): 345203.

DOI: 10.52396/JUSTC-2024-0004
JUSTC, **2024**, 54(6): 0602